Bull. Mater. Sci., Vol. 39, No. 6, October 2016, pp. 1403–1410. © Indian Academy of Sciences.
DOI 10.1007/s12034-016-1289-5

Fabrication of dye-sensitized solar cells with multilayer photoanodes of hydrothermally grown TiO_2 nanocrystals and P25 TiO_2 nanoparticles

MAZIAR MARANDI[1,*], MAHBOUBEH NAEIMI SANI SABET[1] and FARZANEH AHMADLOO[2]
[1]Physics Department, Faculty of Science, Arak University, Arak 38156, Iran
[2]Chemical Engineering Department, Faculty of Engineering, Arak University, Arak 38156, Iran

MS received 10 July 2015; accepted 21 March 2016

Abstract. **TiO_2 nanocrystals (NCs) with sizes around 20 nm were synthesized by hydrothermal method in acidic autoclaving pH. The hydrothermally grown TiO_2 NCs and P25 TiO_2 nanoparticles (NPs) were used in the preparation of two different pastes using different procedures. These pastes with different characteristics were separately deposited on FTO glass plates to form multilayer photoanodes of the dye-sensitized solar cells. The aim of this study was to search how a thin sub-layer of the hydrothermally grown TiO_2 NCs in the photoanodes could improve the efficiency of TiO_2 P25-based solar cells. The highest efficiency of 6.5% was achieved for a cell with a photoanode composed of one transparent sub-layer of hydrothermally grown TiO_2 NCs and two over-layers of P25 NPs. Higher energy conversion efficiencies were also attainable using two transparent sub-layers of hydrothermally grown TiO_2 NCs. In this case, an efficiency of 7.2% was achieved for a cell with a photoelectrode made of one over-layer of P25 TiO_2 NPs. This could show an increase of about 30% in the efficiency compared to the similar cell with a photoanode made of two layers of hydrothermally grown TiO_2 NCs.**

Keywords. **Dye-sensitized solar cells; hydrothermal method; TiO_2 nanocrystals; multilayer photoanodes; energy conversion efficiency.**

1. Introduction

Dye-sensitized solar cells (DSCs) based on nanocrystalline semiconducting oxides and dye sensitizers were introduced by Michael Gratzel in 1991 [1]. These photovoltaic devices have attracted a great deal of attention due to the ease of fabrication, rather than high-energy conversion efficiency and low fabrication costs [1–4]. Among them, DSCs with nanocrystalline TiO_2 photoanodes are vastly investigated [5–12]. Several researches have been performed on dye sensitizers [13–22], structural, optical and electronic properties of the nanocrystalline photoanode [23–25], redox electrolyte [26–29] and counter electrode [30–32]. These investigations could also be classified in two main categories of the photon management, i.e., the increase of the light harvesting efficiency [33–35] and improvement of the electronic properties [25,36]. Fabrication of the photoanodes with perfect nanocrystals (NCs) of the optimized size [37], ideal film preparation [38,39], improvement of the electron transport inside the cell [40–42] and application of light scattering components [43–46] are some important trends of investigations.

There are several reports that demonstrate the application of P25 TiO_2 nanoparticles (NPs) in the photoanode of the DSCs [39,46,47]. It is shown that the prepared P25 films can reveal partial scattering [46–49] and moderate electronic properties [42]. Besides, these NPs are easy to access and could create acceptable efficiencies in combination with other TiO_2 nanostructures [45–48,50]. They could also be used for the formation of the novel TiO_2 structures like nanorods and nanotubes for the application in DSCs [49,50]. In all cases, the optimization of the light harvesting efficiency and electronic properties could result in higher energy conversion efficiencies.

Here TiO_2 NCs with sizes around 20 nm were prepared by hydrothermal method in acidic autoclaving pH. The synthesized NCs and commercially available P25 TiO_2 NPs were applied in the preparation of two different pastes using different procedures. These pastes were separately deposited on the FTO glass substrates to form multilayer photoanodes of DSCs. The main target of the study was to show how a thin transparent sub-layer of hydrothermally grown TiO_2 NCs could improve the efficiency of simple P25 solar cells. The second target was to search for the higher efficiencies for the DSCs with multilayer photoelectrodes. An energy conversion efficiency of 7.2% was achieved for the cell with photoanode made of two transparent sub-layers and one P25 TiO_2 over-layer.

2. Experimental

Hydrothermally grown TiO_2 NCs were synthesized in acidic autoclaving pH [51]. Briefly, 0.035 mol of glacial acetic acid was added to 0.035 mol of titanium tetraiso-propoxide (TTIP) and vigorously stirred. Then 49 ml of DI water was added for the hydrolysis process and the solution was homogenized

*Author for correspondence (m-marandi@araku.ac.ir)

for 1 h. For peptization, a quantity of 0.65 ml of HNO_3 was injected and the sample was refluxed at 80°C for 75 min. The final pale blue solution (pH = 1.4) was transferred to a Teflon-lined stainless steel autoclave and heated at 230°C for 12 h.

For the paste preparation, the aqueous solution of hydrothermally grown TiO_2 NCs was sonicated at first. Then it was concentrated to get a 13 wt% solution of TiO_2 NCs in water. This solution was centrifuged and washed with ethanol for several times. This was repeated to achieve a 40 wt% white precipitate of NCs in ethanol. The total wet TiO_2 precipitate (about 4.7 g) was fully dispersed in proper amount of ethanol using an ultrasonic bath for 20 min. Two other solutions containing terpineol and ethyl cellulose (EC) in ethanol were separately prepared. Two kinds of EC powders, i.e., the EC 5–15 mPas (#46070, Fluka) and EC 15–30 mPas (#46080, Fluka) were used in this stage. The weight percents of these components in total applied EC powder (0.25 g) were about 56 and 44%, respectively. This powder was mixed with about 30 ml of ethanol and stirred. A quantity of 2.027 g of terpineol was also added to 20 ml of ethanol and homogenized. These solutions were slowly added to the TiO_2 NCs sol in ethanol. The final solution was then homogenized by an ultrasonic horn (240 W, 120 × 0.5 s) for three times and concentrated. This was carried out for complete evaporation of the ethanol solvent. The result was a semi-transparent paste of hydrothermally grown TiO_2 NCs composed of 18 wt% TiO_2, 9 wt% EC and 73 wt% of terpineol.

The commercially available P25 TiO_2 NPs were also used for another paste preparation using different methods [52]. A quantity of 0.5 g of P25 TiO_2 powder was transferred to an alumina mortar. Then 0.08 g acetic acid was added and the mixture was ground for 5 min. Later, 0.08 ml of DI water was added and the wet powder was milled for 1 min (this step was repeated 5 times). A quantity of 0.8 ml of ethanol was added and TiO_2 rough paste was ground for 1 min (this step was repeated 15 times). Later, 0.21 ml of ethanol was added and the paste was mixed for 1 min (this step was repeated 6 times). Finally, 8.3 ml of ethanol was added to the solution and the result was transferred to a beaker. The P25 TiO_2 solution was placed in ultrasonic bath and sonicated for 20 min. The other paste preparation steps were performed similar to what was carried out for the hydrothermally grown TiO_2 NCs. The weight percents of the components in P25 TiO_2 paste were repeatedly set to be 18, 9 and 73 wt% for TiO_2, EC and terpineol, respectively.

Multilayer photoanodes of the DSCs were prepared by separate deposition for different pastes on FTO glass substrates. The TiO_2 layers composed of hydrothermally grown NCs were shown by H. The layers composed of P25 TiO_2 NPs were represented as P. The number of the layers deposited by doctor-blade method was also mentioned after the letters H and P. According to the naming rule, different photoanodes of P1, P2, P3, H1, H1P1, H1P2, H1P3 and also H2, H2P1 and H2P2 were prepared and applied in DSCs. The multilayer structures were heated at 325, 375, 450 and 500°C for 5, 5, 15 and 15 min, respectively. Then the dye adsorption was carried out by immersing the photoanodes in an ethanol solution of dye N719 (concentration of 3×10^{-4} M) for 24 h. The other cell fabrication steps, i.e., the preparation of platinum counter electrodes (using 50 mM H_2PtCl_6 solution), cell assembling (by 60 μm thermoplastic spacer), injection of I^-/I_3^- electrolyte and sealing were successively performed.

SEM images of the photoanodes were taken using a T-Scan electron microscope. Optical spectroscopy for the measurement of dye adsorption and transmittance was performed using a Mecasys Optizen system. X-ray diffraction pattern was recorded by a Philips Xpert-pro equipment with Cu Kα (λ = 1.54 Å) radiation. The current–voltage characteristics of the cells were measured under AM 1.5, 100 mW cm^{-2} simulated light radiation. The electrochemical impedance spectroscopy (EIS) was also carried out by an ECO CHEMIE Autolab potentiostat.

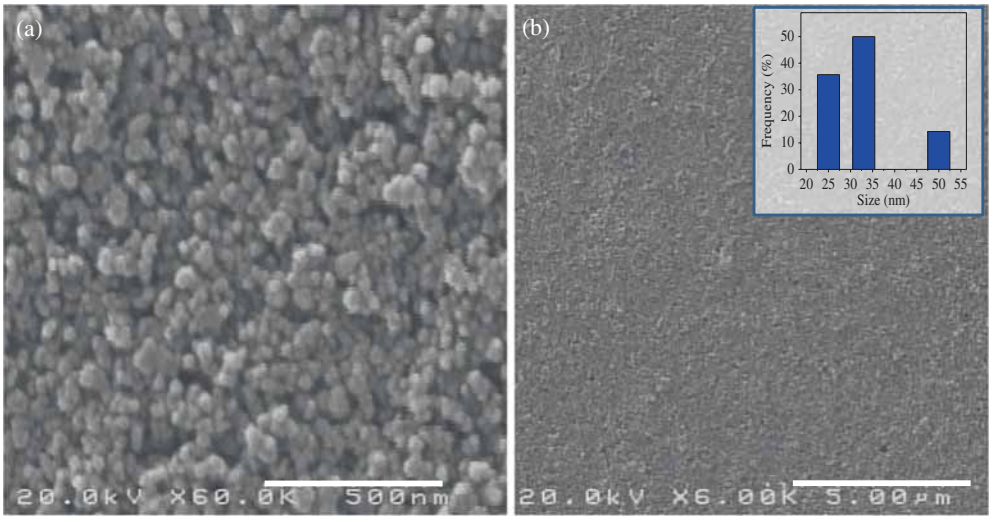

Figure 1. (**a**, **b**) SEM images of the P1 layer composed of P25 TiO_2 nanocrystals in two different magnifications. The size distribution histogram of the particles is shown in inset of **b**.

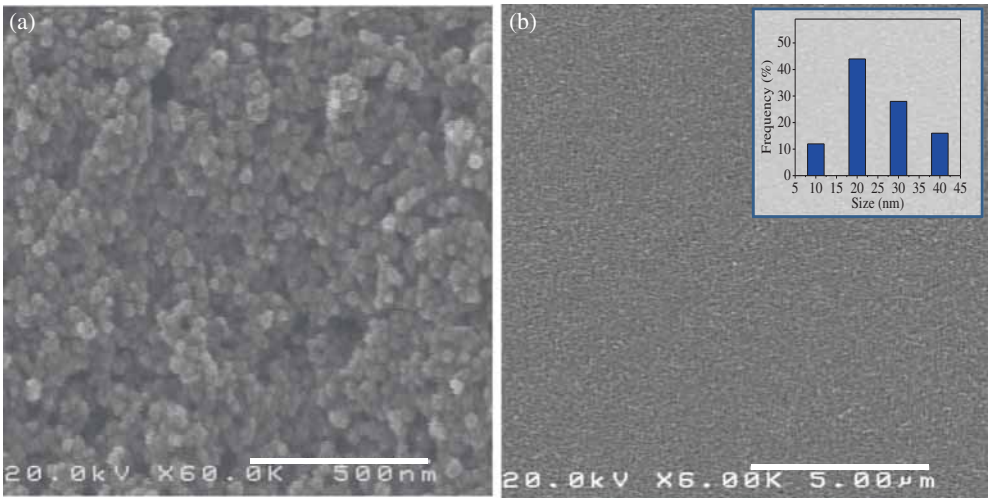

Figure 2. (**a**, **b**) SEM images of the hydrothermally grown TiO_2 nanocrystals in two different magnifications. The size distribution histogram of the nanocrystals is represented in the inset of **b**.

3. Results and discussion

Figure 1 demonstrates SEM images of the P1 layer composed of P25 TiO_2 NPs. As shown in figure 1a, the layer is composed of round shaped TiO_2 NPs with sizes in the range of 25–35 nm. Figure 1b represents the SEM image of the P1 layer in large scale. It could be seen that the layer is uniform and free of cracks on the surface. The size distribution histogram of the NPs is also shown in the inset of figure 1b. It could be observed that most of the particles have sizes around 35 nm. Nevertheless, the appearance of the layer is semi-transparent and nearly white due to the agglomerations.

Figure 2 shows SEM images of the H1 layer composed of hydrothermally grown TiO_2 NCs. As represented in figure 2a, this layer is composed of round TiO_2 NCs with sizes smaller than the P25 TiO_2 NPs. The large-scale SEM image of the H1 layer is also shown in figure 2b. According to the result, the layer is free of cracks and smoother than the P1 layer. This could be attributed to the synthesis method and paste preparation procedure, which do not create agglomerations. The appearance of the layer is also well-transparent and without considerable light scattering. The size distribution histogram of these NCs is represented in the inset of figure 2b. It could be observed that there are particles with sizes in the range of 10–40 nm. Nevertheless, the dominant size of the particles is about 20 nm.

Figure 3 shows the X-ray diffraction pattern (XRD) of the hydrothermally grown TiO_2 NCs. According to the JCPDS card no. 71-1169, the XRD peaks located at 2θ of 25.3°, 37.8°, 48°, 54°, 55.2°, 62.7°, 68.9°, 70.3° and 75.3° belong to the (101), (004), (200), (105), (211), (204), (116), (220) and (215) crystalline planes of the anatase phase of TiO_2, respectively. The average crystallite size of hydrothermally grown TiO_2 NCs could also be estimated using the full-width at half-maximum of the (101) XRD peak and Scherrer formula [53,54]. This size is about 15 nm,

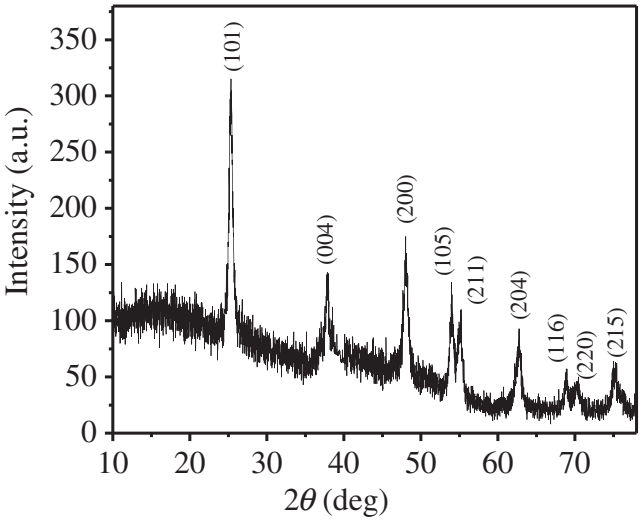

Figure 3. X-ray diffraction pattern of the hydrothermally grown TiO_2 nanocrystals.

which is smaller than the average size achieved from the SEM images.

As mentioned in the experimental section, multilayer structures made of different TiO_2 NCs were deposited on FTO glass substrates to be applied in the photoanode of DSCs. Figure 4 demonstrates the cross-sectional SEM images of the H1P2 and H1P3 multilayer photoelectrodes. It could be seen that there is a compact sub-layer of hydrothermally grown TiO_2 NCs with 3.5 μm thickness on the FTO glass substrates. Besides, it could be observed that the thickness of P2 and P3 over-layers of P25 TiO_2 NPs are about 14.5 and 18 μm, respectively. The thickness of P1 over-layer in H1P1 photoelectrode was measured to be about 10 μm. The simple P1, P2 and P3 photoanodes were also characterized and their thicknesses were about 14.5, 21.5 and 26 μm, respectively. The first category of multilayer photoanodes that were investigated were P1, P2, P3, H1P1, H1P2

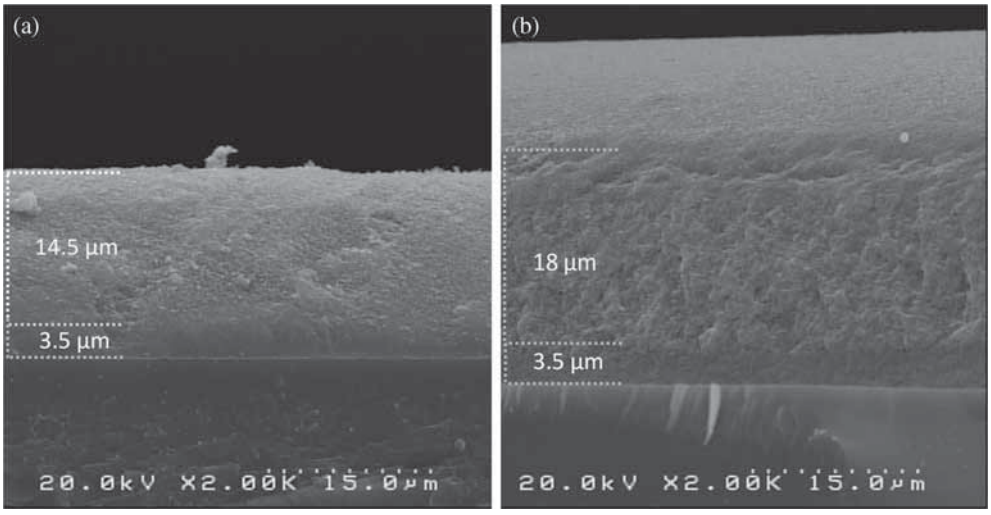

Figure 4. Cross-sectional SEM images of (**a**) H1P2 and (**b**) H1P3 multilayer photoanodes.

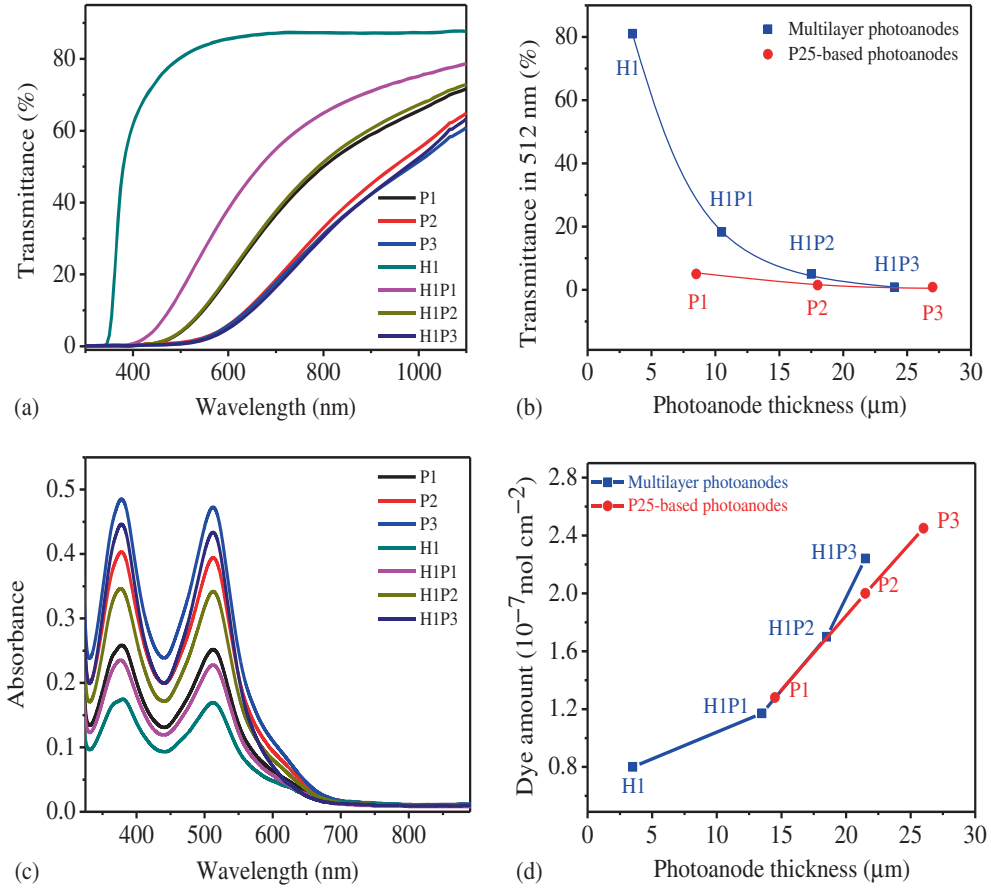

Figure 5. (**a**) Optical transmittance and its corresponding value in 512 nm *vs.* (**b**) the thickness for the P1, P2, P3, H1, H1P1, H1P2 and H1P3 photoelectrodes. (**c**) Absorbance of the dye N719 that is fully desorbed from the surface of the mentioned photoanodes and (**d**) calculated dye loading amount *vs.* the photoanode thickness. Dye desorption process is performed in 3 ml of 0.1 M NaOH solution in a mixed solvent of ethanol and water (water/ethanol = 1:1, v/v).

and H1P3 photoelectrodes. The reason was to search for the curing effect of a thin H1 sub-layer in the photoanode on the performance of the simple P25 solar cells.

Figure 5a demonstrates the transmission spectra of different multilayer photoelectrodes. The corresponding values of transmittance in 512 nm *vs.* the thickness of the photoanodes

are also shown in figure 5b. It could be observed that the transmittance of H1 layer is about 81% in this wavelength. This could confirm that the H1 layer is well-transparent in 4 μm thickness. The similar values of transmittance for P1, P2 and P3 photoanodes were also measured to be about 5, 1.5 and 1%, respectively. As there is no absorption for the TiO_2 layers in 512 nm wavelength, this could show the considerable light scattering of the P25 layers. Besides, the amount of light scattering is increased for the P2 and P3 photoanodes due to the higher thickness. The values of transmittance for H1P1, H1P2 and H1P3 photoanodes in 512 nm were measured to be about 18, 5 and 1%, respectively. It could be seen that the light scattering is increased for higher number of P25 over-layers. Besides, it could be observed that the H1P1 and H1P2 photoanodes are more transparent than the P1 and P2 photoelectrodes. The reason is due to the lower thickness of the P1 and P2 over-layers in H1P1 and H1P2 electrodes compared to those of the P1 and P2 photoanodes.

Figure 5c shows the absorbance of dye N719 solutions, which are fully desorbed from the surface of different multilayer photoanodes. The calculated amounts of the adsorbed dye *vs.* the thickness of different photoanodes are also shown in figure 5d. According to the results, the dye adsorption obviously increased with the thickness for the P1, P2 and P3 photoanodes. The same trend of changes could be observed for the H1, H1P1, H1P2 and H1P3 photoelectrodes. The reason could be attributed to the higher effective surface area of the photoanodes in higher thicknesses. The H1

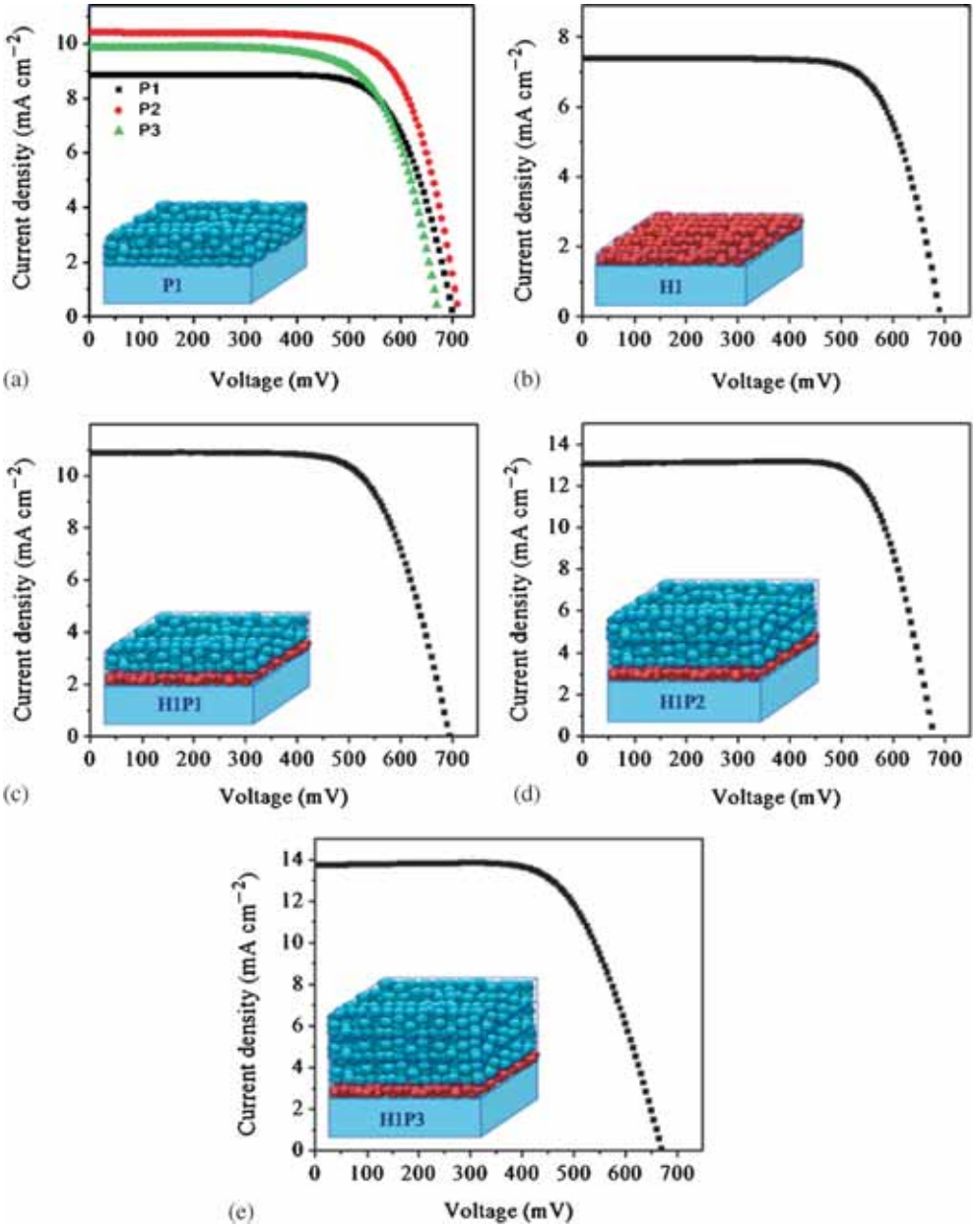

Figure 6. (**a**–**e**) Photocurrent–voltage ($I-V$) characteristics of the dye-sensitized solar cells with H1, P1, P2, P3, H1P1, H1P2 and H1P3 photoelectrodes.

layer represents the lowest amount of dye adsorption, about 0.8×10^{-7} mol cm^{-2}. Besides, the dye loading is lower for the H1P1, H1P2 and H1P3 photoanodes compared to those of the P1, P2 and P3 photoelectrodes, respectively. This is also due to the lower thickness of the P over-layers in H1Px (x = 1–3) photoanodes and their obviously lower total thickness.

Figure 6a–e represents the photocurrent–voltage (I–V) characteristics of DSCs with H1, P1, P2, P3, H1P1, H1P2 and H1P3 photoelectrodes. The photovoltaic parameters of these cells are also summarized in table 1. According to figure 6a, the short-circuit current density (J_{sc}), open-circuit voltage (V_{oc}) and efficiency of the cells with P1, P2 and P3 photoanodes are increased with the thickness. Then they are decreased for the cell with thickest P3 photoelectrode. The measured energy conversion efficiencies were about 4.5, 5.4 and 4.65% for the cells with P1, P2 and P3 photoanodes, respectively. Although the dye loading and light scattering of P3 electrode are higher than those of P1 and P2 photoanodes, the thickness is comparable with electron diffusion length in TiO_2 layer [55–58]. This could obviously increase the electron–hole recombinations and decrease the cell performance. Figure 6b demonstrates the I–V curve of the DSC with H1 photoelectrode. As was previously shown, the 4 μm thick H1 layer was quite uniform and without any cracks on the surface. The layer was well-transparent and tightly bonded to the FTO glass substrates. Besides, the thickness is small and recombination is low for the electrons flowing through this photoanode. As a result, although the corresponding dye loading and light scattering are obviously low, the efficiency was still about 3.7%.

According to the results, the photovoltaic parameters are improved for the DSCs with H1P1, H1P2 and H1P3 multilayer photoanodes. The measured J_{sc} values were about 10.9, 13.3 and 13.7 mA cm^{-2} for the DSCs with H1P1, H1P2 and H1P3 photoanodes, respectively. The energy conversion efficiencies also increased to 5.23, 6.55 and 6.0% for these multilayer photoelectrodes. The lower performance of the DSC with H1P3 photoanode could be attributed to its 24 μm thickness and increased back recombination due to the higher surface area. The maximum efficiency was also achieved for the cell with optimized H1P2 photoelectrode. This value increased to about 21% compared to that of the DSC with P2 photoanode.

Table 1. Photovoltaic parameters of the DSCs with different multilayer photoanodes.

Photoanode structure	J_{sc} (mA cm^{-2})	V_{oc} (mV)	FF	η (%)
H1	7.37	690	0.73	3.71
P1	8.84	705	0.72	4.5
P2	10.41	715	0.72	5.4
P3	9.84	675	0.7	4.65
H1P1	10.88	695	0.69	5.23
H1P2	13.03	675	0.74	6.55
H1P3	13.72	670	0.65	6

As was shown, the dye loading amount and light scattering of P1, P2 and P3 photoanodes were higher than those of the H1P1, H1P2 and H1P3 electrodes, respectively. Consequently, the improved performance of the DSCs with multilayer HP photoanodes could be attributed to the better electronic properties, which are created by H1 sub-layer. This sounds to be related to the lower electron-hole back recombination and better electron transport in the DCSs with improved multilayer photoanodes.

EIS analysis was performed to achieve the electron transport parameters of the H1Px (x = 1–3) photoanodes. Various parameters including the series resistance of the cell (R_S), electron lifetime within the photoanode (τ_{eff}), charge-transfer resistance due to the electron recombination at the TiO_2/electrolyte interface (R_{rec}), chemical capacitance of TiO_2 photoanode (C_μ) and charge-transfer resistance at the interface of counter electrode and electrolyte (R_{CE}) could be extracted.

Figure 7 shows the results of EIS analysis for the cells with H1, H1P1, H1P2 and H1P3 photoanodes. The experiments were carried out in −0.8 V in dark. The inset of the figure demonstrates the equivalent circuit used for the modelling of the impedance data. The theoretical basis and calculation details were delivered and discussed by Adachi *et al* [59]. The corresponding EIS parameters are extracted and summarized in table 2. According to the results, R_s is about 20 Ω for the mentioned cells. Nevertheless, the charge-transfer resistance is quite different. The value of R_{rec} increased from 32.5 Ω for the cell with H1 electrode to 41 Ω and 59 Ω for the cells with H1P1 and H1P2 photoanodes. Then it finally decreased to 43 Ω for the DSC with H1P3 photoelectrode. The chemical capacitance, C_μ, also increased from 364 μF for the H1 photoanode to 376, 454 and 562 μF for the H1P1, H1P2 and H1P3 electrodes, respectively. The calculated electron

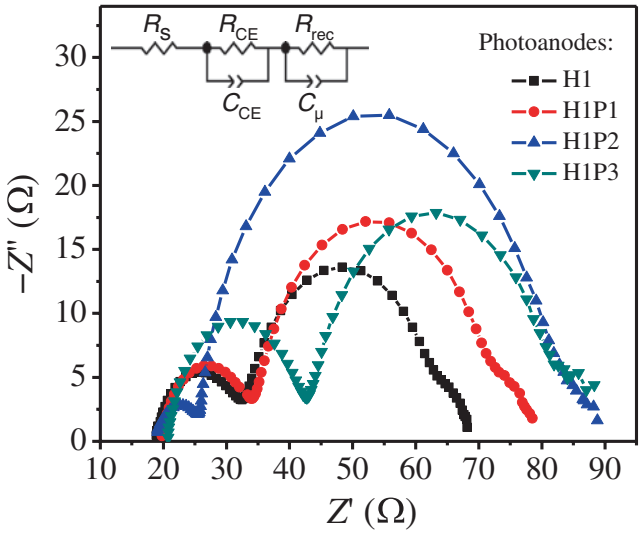

Figure 7. Nyquist plots of the dye-sensitized solar cells with H1, H1P1, H1P2 and H1P3 photoanodes measured at −0.8 V in dark. The inset of the figure shows the equivalent circuit used for modelling of the impedance data.

Table 2. EIS parameters of the dye sensitized solar cells with H1, H1P1, H1P2 and H1P3 photoelectrodes.

Photoanode structure	R_S (Ω)	R_{rec} (Ω)	C (μF)	τ_{eff} (ms)
H1	18.8	32.5	364	12
H1P1	19.9	41	376	16
H1P2	19	59	454	26
H1P3	20	43	562	24

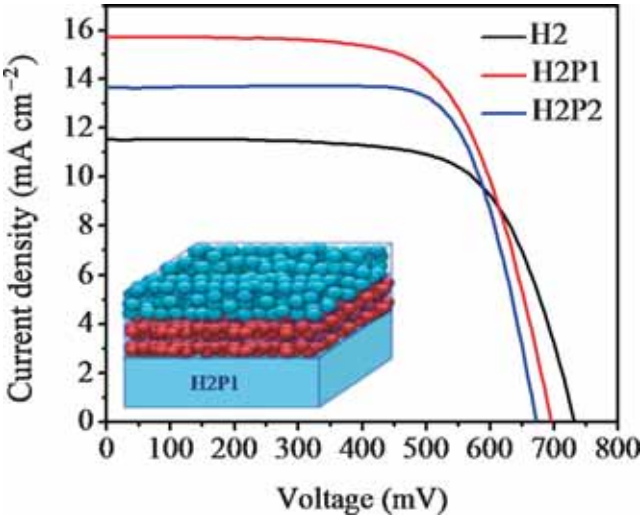

Figure 8. Photocurrent–voltage characteristics of DSCs with multilayer photoanodes of H2, H2P1 and H2P2.

lifetimes related to the H1 and H1Px ($x = 1$–3) photoanodes were about 12, 16, 26 and 24 ms in the same order. It could be seen that the maximum charge-transfer resistance belongs to the cell with H1P2 photoelectrode. Besides, the longest electron lifetime is related to this photoanode too. These two facts are in agreement with better performance of the cell with H1P2 photoelectrode.

Other multilayer photoanodes composed of two transparent sub-layers of hydrothermally grown TiO_2 NCs were also investigated. This was performed for fabrication of some DSCs with higher energy conversion efficiencies. Figure 8 shows the I–V characteristics of the DSCs with H2, H2P1 and H2P2 photoanodes. The photovoltaic parameters of these cells are extracted and summarized in table 3. It could be observed that the photovoltaic performance is obviously improved for the cell with H2P1 photoanode. According to the results, the energy conversion efficiency increased from 5.7% for the cell with H2 photoanode to about 7.2% for the DSC with H2P1electrode. This could show a 30% increase compared to the efficiency of the cell with H2 photoelectrode. The reason could be attributed to the higher amount of dye adsorption and light scattering of the H2P1 photoanode. The energy conversion efficiency slightly decreased for the cell with H2P2 photoelectrode. This could be attributed to the comparable thickness of the photoanode with electron diffusion length in TiO_2 layer.

Table 3. The photovoltaic parameters of DSCs with H2, H2P1 and H2P2 photoelectrodes.

Photoanode structure	J_{sc} (mA cm^{-2})	V_{oc} (mV)	FF	η (%)
H2	11.52	730	0.68	5.7
H2P1	15.69	695	0.66	7.2
H2P2	13.64	670	0.73	6.7

4. Conclusion

DSCs with multilayer photoanodes composed of separate layers of hydrothermally grown TiO_2 NCs and P25 TiO_2 NPs were fabricated. The results demonstrated how a thin sub-layer of hydrothermally grown TiO_2 NCs in the photoanode could obviously increase the efficiency of simple P25 solar cells. The maximum efficiency of 6.55% was achieved for the cell with H1P2 photoanode. This represented a 21% increase compared to the highest efficiency of the cells with just P25 NPs.

Other multilayer photoanodes with two transparent sublayers of hydrothermally grown TiO_2 NCs were also fabricated. A maximum efficiency of 7.2% was achieved for the cell with just one over-layer of TiO_2 P25 NPs. This was about 30% increase compared to the efficiency of the cell with H2 photoanode. The reason was attributed to the higher amount of dye adsorption and light scattering of the P25 TiO_2 over-layer.

References

[1] O'Regan B and Gratzel M 1991 *Nature* **353** 737
[2] Grätzel M 2009 *Acc. Chem. Res.* **42** 1788
[3] Grätzel M 2003 *J. Photochem. Photobiol. C* **4** 145
[4] Grätzel M 2004 *J. Photochem. Photobiol. A* **164** 3
[5] Hagfeldt A, Cappel U B and Boschloo G 2012 *Photovoltaic Solar Energy* **1** 481
[6] Dhungel S K and Park J G 2010 *Renew. Energy* **35** 2776
[7] Ito S, Chen P, Comte P, Nazeeruddin M K, Liska Péchy P and Grätzel M 2007 *Prog. Photovolt: Res. Appl.* **15** 603
[8] Zukalova M, Prochazka J, Zukal A, Yum J H and Kavan L 2008 *Inorg. Chim. Acta* **361** 656
[9] Nazeeruddin M K *et al* 2001 *J. Am. Chem. Soc.* **123** 1613
[10] Shiga T and Motohiro T 2008 *Thin Solid Films* **516** 1204
[11] Lagref J J, Nazeeruddin M K and Grätzel M 2008 *Inorg. Chim. Acta* **361** 735
[12] Giribabu L, Kuma C V, Reddy V G, Reddy P Y, Srinivasa Rao C, Jang S R, Ho Yum J, Nazeeruddin M K and Grätzel M 2009 *J. Chem. Sci.* **121** 75
[13] Horiuchi T, Miura H, Sumioka K and Uchida S 2004 *J. Am. Chem. Soc.* **126** 12218
[14] Lai L F, Qin Ch, Chui Ch H, Islam A, Han L, Ho Ch L and Wong W Y 2013 *Dyes Pigments* **98** 428
[15] Tan L L, Xie L J, Shen Y, Liu J M, Xiao L M, Kuang D B and Su Ch Y 2014 *Dyes Pigments* **100** 269
[16] Awuaha S G, Polreis J, Prakashb J, Qiaob Q and Youa Y 2011 *J. Photochem. Photobiol. A* **224** 116

[17] Caballero R, Barea E M, Fabregat-Santiago F, de la Cruz P, Márquez L, Langa F and Bisquert J 2008 *J. Phys. Chem. C* **112** 18623

[18] Bernard M C, Cachet H, Falaras P, Hugot-Le Goff A, Kalbac M, Lukes I, Oanh N T, Stergiopoulos T and Arabatzis I 2003 *J. Electrochem. Soc.* **150** 155

[19] Klein C, Nazeeruddin M K, Liska P, Censo D D, Hirata N, Palomares E, Durrant J R and Grätzel M 2005 *Inorg. Chem.* **44** 178

[20] Ferber J and Luther J 1998 *Sol. Energy Mater. Sol. Cells* **54** 265

[21] Rothenberger G, Comte P and Grätzel M 1999 *Sol. Energy Mater. Sol. Cells* **58** 321

[22] Usami A 1999 *Sol. Energy Mater. Sol. Cells* **59** 163

[23] Bakhshayesh A M and Mohammadi M R 2013 *Ceram. Int.* **39** 7343

[24] Laskova B *et al* 2012 *Solid State Electrochem.* **16** 2993

[25] Wu J, Lan Z, Hao S, Li P, Lin J, Huang M, Fang L and Huang Y 2008 *Pure Appl. Chem.* **80** 2241

[26] Park S J, Yoo K, Kim J Y, Young Kim J, Lee D K, Kim B S, Kim H, Kim J H, Cho J and Ko M J 2013 *ACS Nano* **7** 4050

[27] Fabregat-Santiago F, Bisquert J, Garcia-Belmonte J, Boschloo J and Hagfeldt A 2005 *Sol. Energy Mater. Sol. Cells* **87** 117

[28] Hauch A and Georg 2001 *Electrochimica Acta* **46** 3457

[29] Mishra A, Fischer M K R and Uerle P B 2009 *Angew. Chem. Int. Ed.* **48** 2474

[30] Murakami T N and Grätzel M 2008 *Inorg. Chim. Acta* **361** 572

[31] Murakami T N, Ito S, Wang Q, Nazeeruddin M K, Bessho T, Cesar I, Liska P, Hu Baker R, Comte P, Péchy P and Grätzel M 2006 *J. Electrochem. Soc.* **153** A2255

[32] Mu Leea K, Chenb Po Y, Hsub Ch Y, Huangb J H, Hoc W H, Chenc H Ch and Hoa K Ch 2009 *J. Power Sources* **188** 313

[33] Tachibana Y, Hara K, Sayama K and Arakawa H 2002 *Chem. Mater.* **14** 2527

[34] Hardin B E, Hoke E T, Armstrong P B, Yum J H, Comte P, Torres T, Fréchet J M J, Nazeeruddin M K, Grätzel M and McGehee M D 2009 *Nat. Photonics* **3** 406

[35] Rodriguez I, Ramiro-Manzano F, Atienzar Martinez J M, Meseguer F, Garcia H and Corma A 2007 *J. Mater. Chem.* **17** 3205

[36] Yanagida S 2006 *C. R. Chimie* **9** 597

[37] Song-Yuan D and Kong-Jia W 2003 *Chin. Phys. Lett.* **20** 953

[38] Zukalova M, Prochazka J, Zukal A, Yum J H and Kavan L 2008 *Inorg. Chim. Acta* **361** 656

[39] DongMei X, ShuJing F, Yuan L, GuoJun D, XuRui X, XuePing L and XiaoWen Z 2007 *Chinese Sci. Bull.* **52** 2481

[40] Bisquert J, Fabregat-Santiago F, Mora-Seró I, Garcia-Belmonte G, Barea E M and Palomares E 2008 *Inorg. Chim. Acta* **361** 684

[41] BeiBei M, Rui G, LiDuo W, YiFeng Z, YanTao S H, Yi G, HaoPeng D and Yong Q 2010 *Sci. China Chem.* **53** 1669

[42] Bakhshayesh A M, Mohammadi M R and Fray D J 2012 *Electrochimica Acta* **78** 384

[43] Koo H J, Park J, Yoo B, Yoo K, Kim K and Park N G 2008 *Inorg. Chim. Acta* **361** 77

[44] Usami A 2000 *Sol. Energy Mater. Sol. Cells* **64** 73

[45] Usami A 1997 *Chem. Phys. Lett.* **277** 105

[46] Barbe Ch J, Arendse F, Comte P, Jirousek M, Lenzmann F, Shklover V and Gratzel M 1997 *J. Am. Ceram. Soc.* **80** 3157

[47] Ito S, Kitamurab T, Wadab Y and Yanagida Sh 2003 *Sol. Energy Mater. Sol. Cells* **7** 3

[48] Lee J K, Jeong B H, Jang S I, Kim Y G, Jang Y W, Lee S B and Kim M R 2009 *J. Ind. Eng. Chem.* **15** 724

[49] Chen Y, Stathatos E and Dionysios D 2009 *J. Photochem. Photobiol. A* **203** 192

[50] Hussain M, Ceccarelli R, Marchisio D L, Fino D, Russo N and Geobaldo F 2010 *Chem. Eng. J.* **157** 45

[51] Ito S, Murakami T N, Comte P, Liska P, Grätzel C, Nazeeruddin M K and Grätzel M 2008 *Thin Solid Films* **516** 4613

[52] Ito S, Chen P, Comte P, Nazeeruddin M K, Liska P, Péchy P and Grätzel M 2007 *Prog. Photovolt. Res. Appl.* **15** 603

[53] Scherrer P 1918 *Mathematisch-Physikalische Klasse* **2** 98

[54] Langford J and Wilson A 1978 *J. Appl. Crystallogr.* **11** 102

[55] Peter L 2007 *J. Electroanal. Chem.* **599** 233

[56] Halme J, Boschloo G, Hagfeldt A and Lund P 2008 *J. Phys. Chem. C* **112** 5623

[57] Peter L M and Wijayantha K G U 2000 *Electrochimica Acta* **45** 4543

[58] Fisher A C, Peter L M, Ponomarev E A, Walker A B and Wijayantha K G U 2000 *J. Phys. Chem. B* **104** 949

[59] Adachi M, Sakamoto M, Jiu J, Ogata Y and Isoda S 2006 *J. Phys. Chem. B* **110** 13872